CrystEngComm

Accepted Manuscript

ROYAL SOCIETY OF CHEMISTRY

www.rsc.org/crystengcomm

CrystEngComm

Dynamic Article Links ►

Cite this: DOI: 10.1039/c0xx00000x

www.rsc.org/CrystEngComm

Article

Surfactant-free synthesis of $SrTiO_3$ hierarchical structures in an ethanol/water mixed solvent at room temperature

Qing-Song Wu, Jian-Wei Liu , Shao-Feng Chen, Hai-Wei Liang and Shu-Hong Yu*

Division of Nanomaterials and Chemistry, Hefei National Laboratory for Physical Sciences at Microscale, Collaborative Innovation Center of Suzhou Nano Science and Technology, Department of Chemistry, University of Science and Technology of China, Hefei, Anhui 230026, P. R. China. Tel: + 86 551 63603040. Email: shyu@ustc.edu.cn

Received (in XXX, XXX) Xth XXXXXXXXX 20XX, Accepted Xth XXXXXXXXX 20XX

DOI: 10.1039/b000000x

Perovskites are a family of important functional materials with excellent ferroelectric, dielectric, pyroelectric, piezoelectric, and electro-optic properties and potential for novel applications. The synthesis methodology for perovskites usually involves harsh conditions. Here, we report a facile new route for synthesis of $SrTiO_3$ hierarchical structures by fast mixing of $SrCl_2{\cdot}6H_2O$ aqueous solution and titanium isopropoxide ethanol solution at room-temperature without using any structure-directing templates. The $SrTiO_3$ particles with different morphologies from cubic to starfish-like hierarchical structures can be prepared, which is strongly dependent on the pH value of the reaction system and the volume ratio of water/ethanol. The formation mechanism of $SrTiO_3$ hierarchical structures has been discussed. This method may provide a green method for synthesis of other perovskite materials in the future.

1. Introduction

Nanomaterials have been widely studied in the past several decades because of their unique size and shape-dependent properties in reduced dimensions.[1] More and more synthesis methods have been introduced to tune the morphology of the nanocrystals. Recently, hierarchical structures have attracted much attention due to their distinct characteristics and potential applications.[2] Various methods have been designed for preparing hierarchical nanomaterials, such as the methods based on vapor-liquid-solid (VLS) mechanism [3] or via vapor transfer and concentration,[4] solvothermal process [5] or reaction in nonaqueous solution,[6] ultrasonic[7] and microwave radiation method,[8] aqueous-phase chemical synthesis[9], bio-inspired approaches.[10] Aqueous-phase chemical synthesis has been considered as a promising route because of its low-energy requirement, environmental benign processing conditions, and the potential for large-scale production.

The perovskite material such as barium titanate ($BaTiO_3$) and strontium titanate ($SrTiO_3$) have excellent ferroelectric, dielectric, pyroelectric, piezoelectric, and electro-optic properties and potential for novel applications, such as electromechanics, dynamic random access memories, capacitors, and nonlinear optics.[11] Several chemical methods have been reported for the preparation of micro- and nano-sized $BaTiO_3$ and $SrTiO_3$ crystals in addition to the standard solid-state method,[12] such as molten salt synthesis,[13] decomposition of bimetallic alkoxide precursors in organic solvents,[14] solvothermal and hydrothermal methods,[15] microwave route, [16] and biosynthesis. [17] Though these routes above offered a successful synthesis of $BaTiO_3$ and $SrTiO_3$ nanoparticles, they usually required temperatures higher than 100 ℃, extreme pH conditions, or expensive reactants. It is highly expected to synthesize these materials at room temperature, ambient pressure, and near-neutral pH, with reactants very accessible and controllable morphology.[18]

Herein, we report a template-free synthesis of hierarchical nanostructures of strontium titanate ($SrTiO_3$) under ambient conditions in an ethanol/water mixed solution. In this approach, $SrCl_2{\cdot}6H_2O$ and titanium isopropoxide were used as reactants. By adjusting the pH value of the initial solution, $SrTiO_3$ nanocrystals with different morphologies from cubic to starfish-like hierarchical structures can be prepared. With the increase of the volume ratio of ethanol/water, the particle size became more uniform and smaller. This versatile strategy provides a new way for synthesis a series of other perovskite ferroelectric materials.

2. Experimental

All chemicals are analytical grade and used as received without further purification. In a typical procedure, $SrCl_2{\cdot}6H_2O$ (1.5 mmol), and a certain amount of KOH were dissolved in 5 mL of deionized water respectively and mixed together to form a homogeneous solution. 1.5 mmol of titanium isopropoxide were dispersed in 10 mL of ethanol (the mole ratio of Sr/Ti = 1). Then, the two solutions were mixed quickly within 20 s under vigorous stirring with immediate formation of a white gelatinous suspension precursor, which was aged at room temperature for a certain time according to the amount of alkali used. The white precipitates were washed by distilled water and absolute ethanol, respectively, and dried in a vacuum at 30 ℃ for 4 h.

X-ray powder diffraction was carried out on the substrate by Philips X'Pert Pro Super Diffratometer CuKα radiation (λ = 1.541874 Å). Scanning electron microscope (SEM) images were obtained by JEOL JSM-6700F and Karl Zeiss Supra 40. Transmission electron microscopy (TEM), high-resolution TEM (HRTEM) and electron diffraction pattern(ED) images were obtained on a JEOL JSM-2010 microscope at an accelerating voltage of 200 kV. Energy-dispersive X-ray (EDX) analysis was obtained with an EDAX detector installed on the same HRTEM.

3. Results and Discussion

3.1 The influence of the concentration of alkali

The thermodynamic modeling work by Riman and co-workers [19] indicated that alkaline-earth titanates and zirconates could be synthesized in aqueous solution even at temperatures below 100 □ when the pH value was appropriate. It is generally believed that high-concentration alkali ($[OH^-] = 1$ mol·dm^{-3}) is required to ensure quantitative precipitation of alkaline-earth titanates. Zhang et al. found the concentration and type of alkali play a key role in the formation of 50-facet Cu_2O microcrystals.[20] Han et al. also reported that different mineralization agents (LiOH and KOH) could adjust the surface structure.[21] In the present study, we found that the concentration of alkali plays a key role in the controllable synthesis of alkaline-earth titanates with various morphologies.

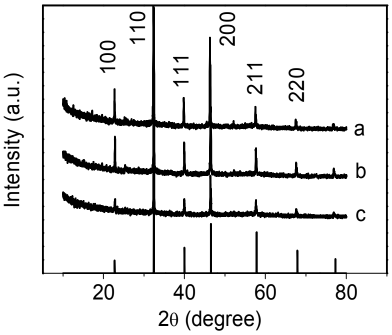

Fig. 1 XRD patterns of the products obtained from the reactions of 1.5 mmol $SrCl_2·6H_2O$ and 1.5 mmol of titanium isopropoxide with various concentration of KOH at room temperature: (a) 2.7 mol·dm^{-3}, (b) 0.9 mol·dm^{-3}, and (c) 0.45 mol·dm^{-3}.

Fig. 1 shows the XRD patterns of the products obtained from the reactions of 1.5 mmol of $SrCl_2·6H_2O$ and 1.5 mmol of titanium isopropoxide with various concentration of KOH at room temperature. All diffraction peaks for these samples can match the standard pattern of cubic $SrTiO_3$ quite well (JCPDS No. 86-0179). No diffraction peaks of $SrCO_3$ or other impurities were found, indicating that the obtained product is pure $SrTiO_3$ without the formation of carbonate. This result reveals that the samples prepared at room temperature using different concentration of KOH are all pure cubic phase $SrTiO_3$.

Fig. 2 shows the SEM and TEM images of $SrTiO_3$ prepared in the presence of 2.7 mol·dm^{-3}, 0.9 mol·dm^{-3}, and 0.45 mol·dm^{-3} KOH, respectively. Well-defined $SrTiO_3$ cubes with a size of ~300 nm were obtained by using 2.7 mol·dm^{-3} KOH (Fig. 2a-c). The surfaces of these cubes were relatively smooth. When the concentration of KOH was reduced from 2.7 mol·dm^{-3} to 0.9 mol·dm^{-3}, eight-pod cubes formed (Fig. 2d-f). The growth orientation tended to <111> axis and the growth of (100) surfaces were limited. Further reducing the concentration of KOH to 0.45 mol·dm^{-3}, the structure becomes more complicated, which was apt to form starfish-like hierarchical structures as shown in Fig. 2g-i. Eight vertices and twelve edge of the cube grow out from the centre, with relatively short and non-contiguous nanorods and nanosheets growing out from them. Then, much shorter nanorods grew on the short ones, leading to a fractal structure. The morphology and size distribution for the different samples were shown in Fig. S1-S3 (ESI†).

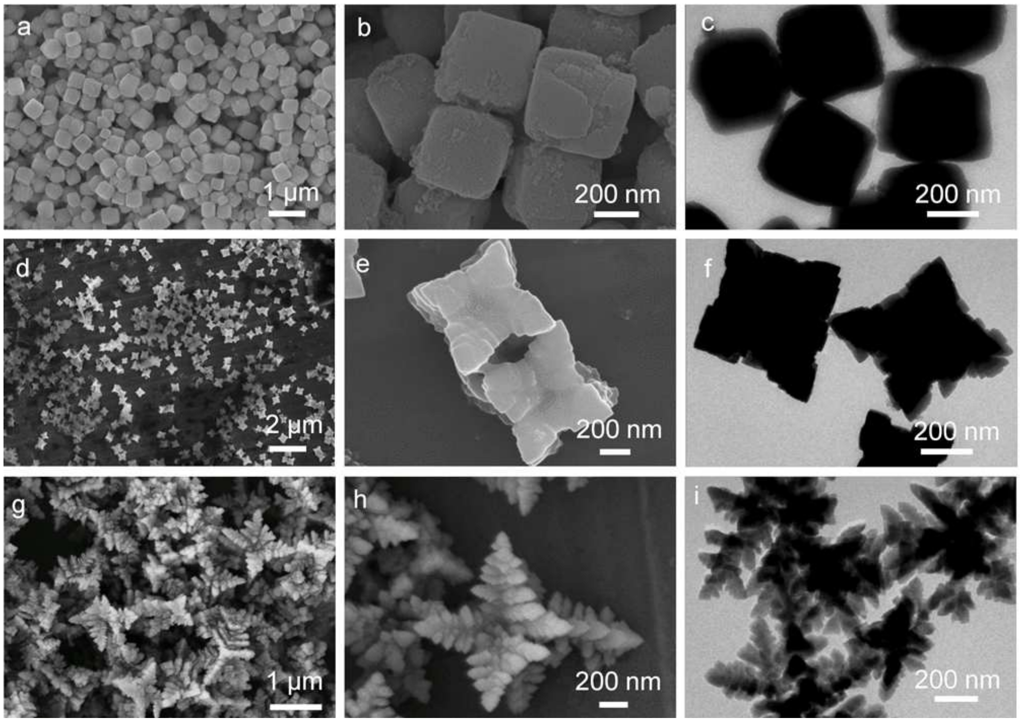

Fig. 2 SEM (a, b, d, e, g, h) and TEM (c, f, j) images of the $SrTiO_3$ samples obtained from the reactions of 1.5 mmol $SrCl_2·6H_2O$ and 1.5 mmol of titanium

isopropoxide with various concentration of KOH at room temperature: (a, b, c) 2.7 mol·dm^{-3}, (d, e, f) 0.9 mol·dm^{-3}, and (g, h, i) 0.45 mol·dm^{-3}

The lattice fringes observed in the HRTEM images and the ED patterns confirm that all samples are single crystalline (Fig. 3). The distance between adjacent lattice fringes in the HRTEM images of hexagonal and starfish-like structure were measured to be 0.276 nm and 0.277 nm, respectively, which were very closed to the standard lattice spacing of the [110] planes of cubic $SrTiO_3$, i.e. 0.275 nm. According to the HRTEM images and ED patterns (Fig. 3), it can be confirmed that the growing orientation of the eight vertices was along the <111> axis. In addition, the energy dispersive X-ray spectroscopy (EDS) indicated that the molar radio of Sr:Ti is near 1:1 (ESI†, Fig. S4).

The influence of the concentration of [OH^-] on the morphology of the particles has been investigated. Usually, we can get two ideal surface terminations if we cleave the bulk crystal of $SrTiO_3$ along any Miller Index plane. Therefore, $SrTiO_3$-(100) plane can have a SrO-terminated and a TiO_2-terminated surface. The $SrTiO_3$-(110) surface consists of alternating O_2^{4-} and $SrTiO^{4+}$ layers and the $SrTiO_3$-(111) surface consists of alternating SrO_3^{4-} and Ti^{4+} layers (Fig. 4). Thus, the (100) planes are non-polar surfaces. The (110) and (111) planes are called polar surfaces. The stabilization of polar surfaces needs a modification of the surface layer charges.[22] From Fig. 4, we can see the range of absorption capacity for [OH^-] is (111) > (110) > (100). The (111) planes need more [OH^-] to maintain the stabilization than (110) and (100) planes. If the concentration of [OH^-] is high enough, all surfaces are covered by anions, thus the $SrTiO_3$ crystal will grow according to its cubic structure. With decreasing the concentration of [OH^-], the stabilization capacity of anions to (111) planes declined, but the (110) planes still maintain a certain stability. The growth through the (110) and (100) axis was still impeded, and the limitation of the crystal growth along (111) axis was weaker and weaker, which forms the star-like morphology. According to the report by Noguera et al,[23] the (110) face of cubic $SrTiO_3$ is considered to be the one of the most energetically stable crystal face, similar to the (100), which explained why the {110} orientations can be quite easily obtained for $SrTiO_3$.

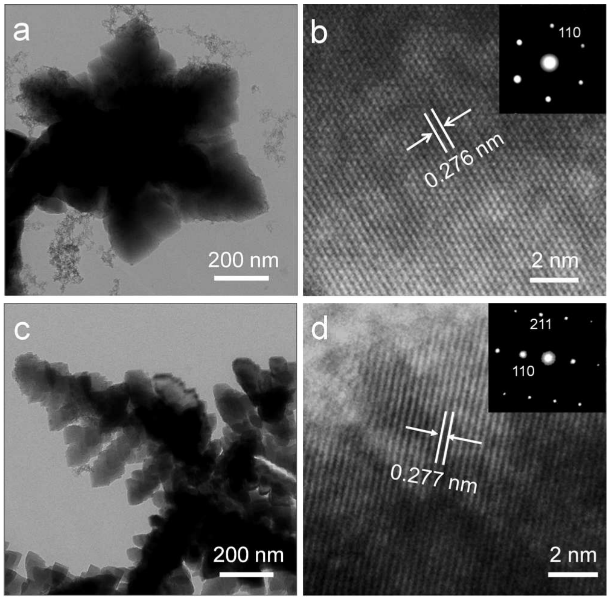

Fig. 3 High-magnification TEM (a, c) and HRTEM (b, d) images of the $SrTiO_3$ samples prepared using different concentration of KOH. (a, b) 0.9 mol·dm^{-3} and (c, d) 0.45 mol·dm^{-3}. The insets in HRTEM images show the corresponding ED patterns.

The concentration of [OH^-] not only could control the final morphology but also could influence the crystallization rate. The higher of the concentration of [OH^-], the faster crystallization rate is. With the presence of 2.7 mol·dm^{-3} KOH, the suspension could totally precipitate in less than 2 h. We could slow down the crystallization process by reduce the concentration of [OH^-]. With the presence of 0.45 mol·dm^{-3} KOH, the complete precipitation process will need 4~5 days.

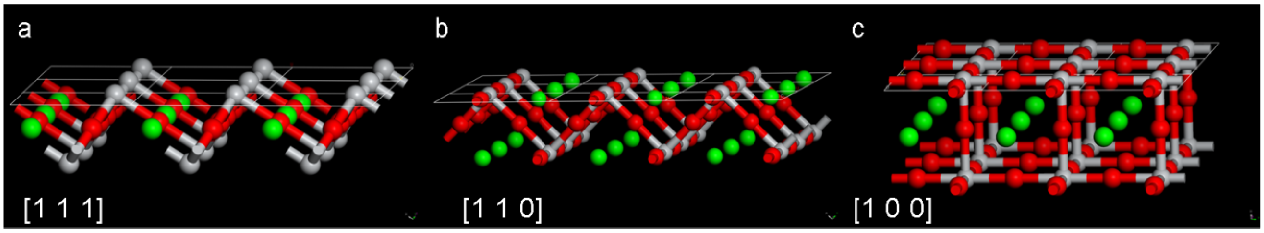

Fig. 4 Atom packing models on different basal equivalent crystal plane families surfaces of cubic $SrTiO_3$. (a) Packing model on the {111} equivalent crystal plane families surfaces. View along the (111) surface. (b) Packing models on the {110} equivalent crystal plane families surfaces. View along the (110) surface. (c) Packing models on the {100} equivalent crystal plane families surfaces. View along the (100) surface. Green spheres present Sr atoms. Red spheres present O atoms. Gray spheres present Ti atoms.

3.2 The influence of volume ration of water/ethanol

Previously, we found that the water content in a mixed water/ethanol solvent has great influence on morphology and phase of $CeOHCO_3$[24] and $CaCO_3$.[25] In order to further understanding the role of ethanol concentration, the volume ratio of ethanol in mixed solvent was varied from 0 to 75v/v% while maintain the whole volume constant.

The XRD pattern in Fig. 5d shows that the final products prepared in solutions with different volume ratio of water/ethanol were still pure cubic phase $SrTiO_3$. Thus, the concentration of ethanol did not influence on the phase of final products. In pure water system, we found that the rate of hydrolysis was too fast in aqueous solution and the precipitate formed within 5 min, so that it is hard to get the particles with unique shape and uniform sizes (Fig. 5a). However, in the presence of ethanol, the rate of hydrolysis of titanium isopropoxide can be tuned. The nucleation process was more homogeneous and the particle size could be more uniform (Fig. 5b, c). By increasing the concentration of ethanol in this system, the particle size can be reduced from 500 nm to ~150 nm.

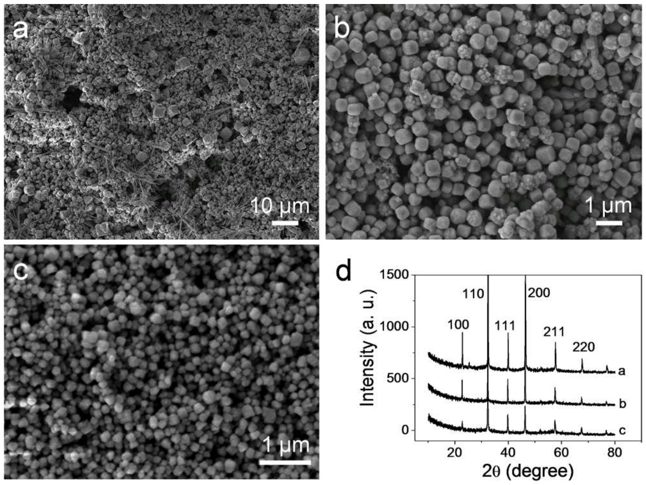

Fig. 5 SEM images of the $SrTiO_3$ samples obtained with different water/ethanol ratio in 2.7 mol·dm^{-3} KOH: (a) pure water, (b) water: ethanol = 3:1, and (c) water: ethanol = 1:3, (d). XRD patterns of the samples obtained with different water/ethanol ratio in 2.7 mol·dm^{-3} KOH.

From Fig. S5–S6 (ESI†), it was found that the laws above were still effective. Though the final phase of products were pure cubic $SrTiO_3$, the morphology was changed. With the absence of ethanol, the morphology of sample was messy. While the volume ratio of ethanol increased to 25%, the starfish-like structure came back but the particle size was close to 1 µm. When the volume ratio of ethanol increased to 75%, the crystal size decreased to ~100 nm, associated with lots of nanoparticles without any special morphology. In solution system, a low supersaturation degree brings on inhomogeneous nucleation, which results in less uniformity of final crystal; while a high supersaturation degree leads to homogeneous nucleation, which makes crystal grow evenly. [26] During the formation of nanocrystalline, the competition between the crystal growth and the nucleation always exists and was controlled by diffusion. The diffusion of particles is more difficult in solutions of high viscosity, which tends to the formation and crystallization of new nuclei. Due to ethanol has a higher viscosity than water, the mixed solution with higher ethanol contents would form crystals of smaller size. A similar phenomenon was reported by Yu and co-workers previously.[27] In this experiment, with the increase of concentration of ethanol, the ion supersaturation degree and viscosity of solution system raised. It's easy to comprehend why the particles size become more uniform and smaller.

3.3 The formation of hierarchical structure

In order to learn the growth mechanism of the hierarchical structure, a series of time-dependent examinations were investigated. Fig. 6d shows the XRD patterns of products gathered at different times in 2.7 mol·dm^{-3} KOH. At 5 min, there is no peak appeared in the pattern, which shows the product was amorphous nanoparticles. At 1 h, the XRD pattern shows some peaks corresponding to the (110) and (200) faces. With the time prolong, the crystallization process became more thoroughly. The TEM images shown in Fig. 6a-c proved this process. At the beginning there were only amorphous nanoparticles, then, crystalline cubes formed. The whole process obeys the Oswald ripening progress. Small amorphous nanoparticles forms and they further agglomerate or dissolve, re-crystallize, to finally form crystalline cubes.

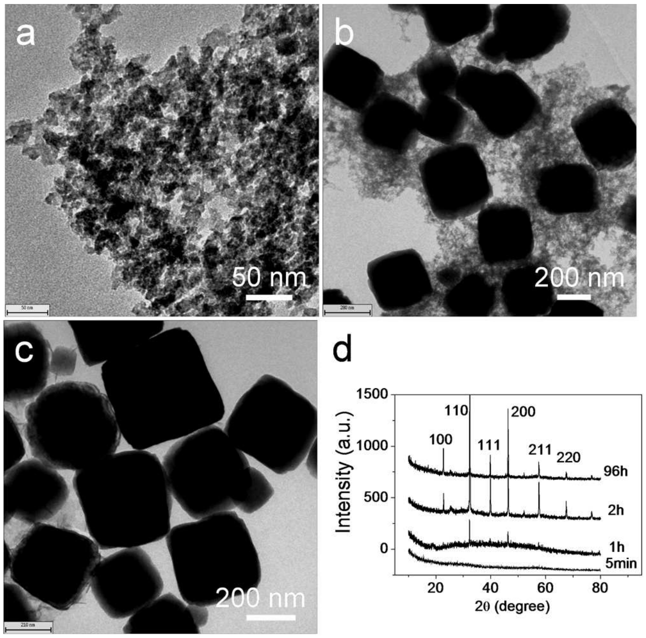

Fig. 6 TEM images of the samples obtained by using 2.7 mol·dm^{-3} KOH with different reaction time: (a) 5 min, (b) 24 h, and (c) 96 h. (d) XRD patterns of the samples obtained by using 2.7 mol·dm^{-3} KOH with different reaction time.

The similar phenomena were also observed while the concentration of alkali reduced to 0.9 mol·dm^{-3} and 0.45 mol·dm^{-3} (ESI†, Fig. S7–S10). Amorphous nanoparticles were checked by XRD (ESI†, Fig. S7, S9) and TEM (ESI†, Fig. S8, S10) when the reaction was stopped after 5 minutes. With the time prolong to 5 hours, some big crystals formed (ESI†, Fig. S8, S10). As discussed in section 3.1 based on adsorption of [OH-] on (111), (110) and (100) crystal faces, comparing with formation of the $SrTiO_3$ cubes at high concentration of [OH-] due to inhibition of crystal growth along <111> direction, the $SrTiO_3$ crystals tends to grow along <111> direction to form eight-branch structures with exposed [110] faces by consumption of amorphous nanoparticles. The quantity of amorphous nanoparticles decreased obviously after one day's aging, while it as feedstock for growth of hierarchical structure was disappeared after aging for 5 days (ESI†, Fig. S7-S10). Furthermore, the lower concentration of [OH-] anions (0.45 mol·dm^{-3}) leads the $SrTiO_3$ crystals to grow along <111> direction enough to form dendritic hierarchical structure.

4. Conclusion

In summary, we have developed a very simple strategy for preparing hierarchical nanostructure of strontium titanate ($SrTiO_3$) under ambient ethanol/water mixed solution at room-temperature. The nanocrystals were synthesized by fast mixing of

$SrCl_2·6H_2O$ water solution and titanium isopropoxide ethanol solution in a jar, without any surface-capping molecules or structure-directing templates. A series reaction conditions were adjusted to study the mechanism of the process. The results showed that the pH value played a key role in controlling the final morphologies of single crystalline $SrTiO_3$ particles. In addition, the concentration of ethanol in mixed solution could control the rate of hydrolysis and nucleation. Time-dependent reaction revealed that the formation of nanocrystal obey the Oswald-ripening process. The present reaction system offers an easy route to synthesize single crystalline $SrTiO_3$ under mild condition at room temperature, and this strategy will be extended to synthesize other perovskite ferroelectric materials.

Acknowledgement

We acknowledge the special funding support from the Ministry of Science and Technology of China, the National Basic Research Program of China (Grants 2013CB933900, 2014CB931800), and the National Natural Science Foundation of China (Grants 21401183, 21431006, 91022032).

† Electronic Supplementary Information (ESI) available: [details of any supplementary information available should be included here]. See DOI: 10.1039/b000000x/

References

1 (a) Y. Yin and A. P. Alivisatos, *Nature,* 2005, **437**, 664. (b) W. L. Noorduin, A. Grinthal, L. Mahadevan and J. Aizenberg, *Science*, 2013, **340**, 832.

2 (a) Z. W. Pan, S. M. Mahurin, S. Dai and D. H. Lowndes, *Nano Lett.*, 2005, **5**, 723. (b) M. H. Cao, T. F. Liu, S. Gao, G. B. Sun, X. L. Wu, C. W. Hu and Z. L. Wang, *Angew. Chem. Int. Ed.*, 2005, **44**, 4197. (c) R. Bardhan, O. Neumann, N. Mirin, H. Wang and N. J. Halas, *ACS Nano*, 2009, **3**, 266. (d) V. Polshettiwar, B. Baruwati and R. S. Varma, *ACS Nano*, 2009, **3**, 728. (e) L. Shang, C. Zhou, T. Bian, H. J. Yu, L. Z. Wu, C. H. Tung and T. R. Zhang, *J. Mater. Chem. A*., 2013, **1**, 4552.

3 (a) Z. L. Wang and Z. W. Pan, *Adv. Mater.*, 2002, **14**, 1029. (b) K. A. Dick, K. Deppert, M. W. Larsson, T. Martensson, W.Seifert, L. R. Wallenberg and L. Samuelson, *Nat. Mater.*, 2004, **3**, 380. (c) J. P. Ge and Y. D. Li, *Adv. Funct. Mater.*, 2004, **14**, 157.

4 (a) H. Q. Yan, R. R. He, J. Johnson, M. Law, R. J. Saykally and P. D. Yang, *J. Am. Chem. Soc.*, 2003, **125**, 4728. (b) Z. L. Wang, X. Y. Kong and J. M. Zuo, *Phys. Rev. Lett.*, 2003, **91**, 185502. (c) Z. L. Wang, X. Y. Kong, Y. Ding, P. X. Gao, W. L. Hughes, R. S. Yang and Y. Zhang, *Adv. Funct. Mater.*, 2004, **14**, 943. (d) J. H. Park, H. J. Choi, Y. J. Choi, S. H. Sohn and J. G. Park, *J. Mater. Chem.*, 2004, **14**, 35.

5 (a) Q. Peng, Y. J. Dong, Z. X. Deng and Y. D. Li, *Inorg. Chem.*, 2002, **41**, 5249. (b) D. B. Kuang, A. W. Xu, Y. P. Fang and H. Q. Liu, *Adv. Mater.*, 2003, **15**, 1747. (c) J. P. Zhu, S. H. Yu, Z. B. He, J. Jiang, K. Chen and X. Y. Zhou, *Chem. Commun.*, 2005, **46**, 5802.

6 (a) A. G. Kanaras, C. Sonnichsen, H. T. Liu and A. P. Alivisatos, *Nano Lett.*, 2005, **5**, 2164. (b) A. Naravanaswamy, H. F. Xu, N. Pradhan and X. G. Peng, *Angew. Chem. Int. Ed.*, 2006, **45**, 5361.

7 J. P. Xiao, Y. Xie, R. Tang, M. Chen and X. B. Tian, *Adv. Mater.*, 2001,**13**, 1887.

8 Y. H. Ni, H. J. Liu, F. Wang, Y. Y. Liang, J. M. Hong, X. Ma and Z. Xu, *Cryst. Growth Des.*, 2004, **4**, 759.

9 (a) H. Cölfen and S. Mann, *Angew. Chem. Int. Ed.*, 2003, **42**, 2350. (b) H. T. Shi, L. M. Qi, J. M. Ma, H. M. Cheng and B. Y. Zhu, *Adv. Mater.*, 2003, **15**, 1647. (c) B. Liu, S. H. Yu, L. J. Li, Q. Zhang, F. Zhang and K. Jiang, *Angew. Chem. Int. Ed.*, 2004, **43**, 4745. (d) T. R. Zhang, W. J. Dong, M. Keeter-Brewer, S. Konar, R. N. Njabon and Z. R. Tian, *J. Am. Chem. Soc.*, 2006, **128**, 10960. (e) H.B. Chu, X. M. Li, G. D. Chen, Z. Jin, Y. Zhang and Y. Li, *Nano Res.*, 2008, **1**, 213.

10 C. Sanchez, H. Arribart and M. M. G. Guille, *Nat. Mater.*, 2005, **4**, 277.

11 (a) S. O'Brien, L. Brus and C. B. Murray, *J. Am. Chem. Soc.*, 2001, **123**, 12085. (b) W. S. Yun, J. J. Urban, Q. Gu and H. Park, *Nano Lett.*, 2002, **2**, 447. (c) K. J. Choi, M. Biegalski, Y. L. Li, A. Sharan, J. Schubert, R. Uecker, P. Reiche, Y. B. Chen, X. Q. Pan, V. Gopalan, L. Q. Chen, D. G. Schlom and C. B. Eom, *Science*, 2004, **306**, 1005.

12 T. Toshima, H. Ishikawa, S. Tanda and T. Akiyama, *Crystal Growth & Design*, 2008, **8**, 2066.

13 (a) H. Liu, C. G. Hu and Z. L. Wang, *Nano Lett.*, 2006, **6**, 875. (b) Y. Mao, S. Banerjee and S. S. Wong, *J. Am. Chem. Soc.*, 2003, **125**, 15718.

14 (a) J. J. Urban, W. S. Yun, Q. Gu and H. Park, *J. Am. Chem. Soc.*, 2002, **124**, 1186. (b) R. L. Brutchey and D. E. Morse, *Angew. Chem. Int. Ed.*, 2006, **45**, 6564. (c) N. Nuraje, K. Su, A. Haboosheh, Nan-loh Yang and H. Matsui, *Adv. Mater.*, 2006, **18**, 807.

15 (a) M. Leoni, M. Viviani, P. Nanni and V. Buscaglia, *J. Mater. Sci. Lett.*, 1996, **15**, 1302. (b) X. Wang, J. Zhuang, Q. Peng and Y. D. Li, *Nature*, 2005, **437**, 121. (c) U. A. Joshi and J. S. Lee, *Small*, 2005, **1**, 1172. (d) M. Niederberger, G. Garnweitner, N. Pinna and M. Antonietti, *J. Am. Chem. Soc.*, 2004, **126**, 9120. (e) L. Q. Dong, H. Shi, K. Cheng and W. Q. Han, *Nano Research*, 2014, **7**, 1311. (f) V. Kalyani, B. S. Vasile, A. Ianculescu, M. T. Buscaglia, V. Buscaglia and P. Nanni, *Cryst. Growth Des.*, 2012, **12**, 4450. (g) W. J. Dong, B. J. Li, Y. Li, X. B. Wang, L. N. An, C. R. Li, B. Y. Chen, G. Wang and Z. Shi, *J. Phys. Chem. C*, 2011, **115**, 3918.

16 (a) E. K. Nyutu, C. H. Chen, P. K. Dutta and S. L. Suib, *J. Phys. Chem. C*, 2008, **112**, 9659. (b) M. L. Moreira, G. P. Mambrini, D. P. Volanti,□ E. Longo□ and J. A. Varela, *Chem. Mater.*, 2008, **20**, 5381. (c) Y. Ma, E. Vileno, S. L. Suib and P. K. Dutta, *Chem. Mater.*, 1997, **9**, 3023. (d) A. E. Souza, G. T. A. Santos, B. C. Bara, W. D. Macedo, Jr., S. R. Teixeira, C. M. Santos, A. M. O. R. Senos, L. Amaral and E. Longo, *Cryst. Growth Des.*, 2012, **12**, 5671.

17 V. Bansal, P. Poddar, A. Ahmad and M. Sastry, *J. Am. Chem. Soc.*, 2006, **128**, 11958.

18 (a) W. B. Christopher, A. C. Marie and R. L. Brutchey, *Small*, 2008, **4**, 2102. (b) K. Su, N. Nuraje and N. L. Yang, *Langmuir*, 2007, **23**, 11369.

19 (a) M. M. Lencka and R. E. Riman, *Chem. Mater.*, 1993, **5**, 61. (b) M. M. Lencka and R. E. Riman, *J. Am. Ceram. Soc.*, 1993, **76**, 2649. (c) M. M. Lencka and R. E. Riman, *Chem. Mater.*, 1995, **7**, 18. (d) M. M. Lencka, E. Nielsen, A. Anderko and R. E. Riman, *Chem. Mater.*, 1997, **9**, 1116.

20 Y. H. Liang, L. Shang, T. Bian, C. Zhou, D. H. Zhang, H. J. Yu, H. T. Xu, Z. Shi, T. R. Zhang, L. Z. Wu and C. H. Tung, *CrystEngComm*, 2012, **14**, 4431.

21 L. Q. Dong, K. Cheng, W. J. Weng and W. Q. Han, *CrystEngComm*, 2014, DOI: 10.1039/C4CE01978D.

22 A. Asthagiri and D.S. Sholl, *Surface Science*, 2005, **581**, 66.

23 (a) F. Bottin, F. Finocchi and C. Noguera, *Phys. Rev. B*, 2003, **68**, 035418. (b) M. Miyauchi, *J. Phys. Chem. C*, 2007, **111**, 12440.

24 S. F. Chen, S. H. Yu, J. Jiang, F. Q. Li and Y. K. Liu, *Chem. Mater.*, 2006, **18**, 115.

25 S. F. Chen, S. H. Yu, B. Yu, L. Ren, W. T. Yao and H. Cölfen, *Chem. Eur . J.*, 2004, **10**, 3050.

26 T. X. Wang, A. W. Xu and H. Cölfen, *Angew. Chem. Int. Ed.*, 2006, **45**, 4451.

27 J. C. Yu, L. Zhang, Q. Li, K. W. Kwong, A. W. Xu and J. Lin, *Langmuir*, 2003, **19**, 7673.

TOC

$SrTiO_3$ hierarchical structures can be synthesized in an ethanol/water mixed solvent at room temperature without using any structure-directing templates.